



# Observation of Longitudinal Magnetic Fluctuations at a First-Order Ferromagnetic Quantum Phase Transition in $\text{UGe}_2$

Noma, Yuichiro ; Kotegawa, Hisashi ; Kubo, Tetsuro ; Tou, Hideki ; Harima, Hisatomo ; Haga, Yoshinori ; Yamamoto, Etsuji ; Ōnuki,...

---

(Citation)

Journal of the Physical Society of Japan, 90(7):073707

(Issue Date)

2021-07-15

(Resource Type)

journal article

(Version)

Accepted Manuscript

(Rights)

©2021 The Physical Society of Japan

(URL)

<https://hdl.handle.net/20.500.14094/0100481848>



## Observation of Longitudinal Magnetic Fluctuations at a First-Order Ferromagnetic Quantum Phase Transition in $\text{UGe}_2$

Yuichiro Noma<sup>1</sup>, Hisashi Kotegawa<sup>1\*</sup>, Tetsuro Kubo<sup>2</sup>, Hideki Tou<sup>1</sup>, Hisatomo Harima<sup>1</sup>,  
Yoshinori Haga<sup>3</sup>, Etsuji Yamamoto<sup>3</sup>, Yoshichika Ōnuki<sup>4</sup>, Kohei M. Itoh<sup>5</sup>,  
Ai Nakamura<sup>6</sup>, Yoshiya Homma<sup>6</sup>, Fuminori Honda<sup>6</sup>, Dai Aoki<sup>6</sup>

<sup>1</sup>*Department of Physics, Kobe University, Kobe 657-8501, Japan*

<sup>2</sup>*Department of Applied Physics, Okayama University of Science, Okayama 700-0005, Japan*

<sup>3</sup>*Advanced Science Research center, Japan Atomic Energy Agency, Tokai, Ibaragi 319-1195, Japan*

<sup>4</sup>*RIKEN Center for Emergent Matter Science, Wako, Saitama 351-0198, Japan*

<sup>5</sup>*School of Fundamental Science and Technology, Keio University, Yokohama 223-8522, Kanagawa, Japan*

<sup>6</sup>*Institute for Materials Research, Tohoku University, Oarai 311-1313, Ibaraki, Japan.*

The connection between ferromagnetic (FM) fluctuations and superconductivity has been well established in FM superconductors  $\text{UCoGe}$  and  $\text{URhGe}$ . However, this connection has not been clarified in  $\text{UGe}_2$ , in which pressure-induced superconductivity emerges in the FM phase. We show results focusing on the spin-echo decay rate,  $1/T_2$ , obtained using  $^{73}\text{Ge}$ -nuclear magnetic resonance (NMR) under pressure, which reveals longitudinal magnetic fluctuations in  $\text{UGe}_2$ . These fluctuations originate in a FM critical point located at a nonzero temperature and developed near the first-order FM quantum phase transition. This remarkable feature at the high-pressure side, where a superconducting anomaly has been clearly observed, provides a connection of FM fluctuations and superconductivity in  $\text{UGe}_2$ . This strongly supports a consensus that superconductivity in ferromagnets is universally mediated by anisotropic magnetic fluctuations.

Emergence of superconductivity in ferromagnets was first observed in  $\text{UGe}_2$  two decades ago.<sup>1)</sup> This finding countered the concept that magnetized materials do not favor superconductivity and pioneered the field of ferromagnetic (FM) superconductivity. The discovery of superconductivity in  $\text{URhGe}$  and  $\text{UCoGe}$  have further expanded this field,<sup>2,3)</sup> especially in studies of field-induced or enhanced superconductivity.<sup>4,5)</sup> It is still under consideration whether a recently discovered superconductor,  $\text{UTe}_2$ ,<sup>6)</sup> is in this same class, but the strong enhancement of its superconductivity under magnetic fields is reminiscent of a FM superconductor.<sup>7,8)</sup> Studies in these systems have clearly demonstrated that superconductivity grows under substantial polarization of magnetic moments. The formation of Cooper pairs is promoted and accompanied by degeneracy-lifting of the Fermi surfaces, which deviates from conventional theory of superconductivity based on electron-phonon interaction.

Many experimental and theoretical investigations have promoted understanding of superconducting mechanism in ferromagnets.<sup>9,10)</sup> Among them, FM fluctuations are regarded as the most likely driving force to bind magnetically polarized electrons into a Cooper pair. A firm connection of superconductivity and FM fluctuations was first shown in  $\text{UCoGe}$ .<sup>11)</sup> Ising-like magnetic fluctuations, observed by nuclear magnetic resonance (NMR) measurements, were coupled with superconductivity. This is qualitatively consistent with the idea of induced superconductivity in a ferromagnet, which had been proposed before the discovery of FM superconductors.<sup>12)</sup> A naive and crucial question is whether this connection is universal among all related superconductors. Subsequently, in  $\text{URhGe}$ , a similar connection has also been established for the field-induced superconductivity. As shown in Fig. 1(a), the magnetic field perpendicular to the easy axis

suppresses the FM phase of  $\text{URhGe}$  and the second-order FM transition changes to a first order just below  $H_R$ , around which reentrant superconductivity appears.<sup>13–16)</sup> The NMR relaxation rates show divergent behavior near  $H_R$ <sup>14,17)</sup> and are strongly coupled with superconductivity against tilting the magnetic field.<sup>17,18)</sup> In  $\text{URhGe}$ , the link between magnetic correlations and superconductivity has also been suggested from electron-electron scattering in resistivity and electronic specific heat.<sup>19,20)</sup> In  $\text{UTe}_2$ , as shown in Fig. 1(b), superconductivity is remarkably enhanced toward the first-order metamagnetic transition at  $H_m$ .<sup>7,8,21,22)</sup> Electron-electron scattering in resistivity and the derived electronic specific heat are strongly enhanced near  $H_m$ ,<sup>21,22)</sup> suggestive of the contribution of magnetic fluctuations induced at the phase boundary to superconductivity.

The phase diagrams of  $\text{URhGe}$  and  $\text{UTe}_2$  are analogous to that of  $\text{UGe}_2$ , which is shown in Fig. 1(c). Here, a control parameter (the horizontal axis) is replaced by pressure and a paramagnetic (PM) phase and two different FM phases, FM1 and FM2, appear. Superconductivity is induced in the vicinity of the first-order FM1-FM2 boundary, at  $P_x \sim 1.2$  GPa, where spontaneous magnetic polarization is changed by pressure. In all three systems in Fig. 1, regardless of the difference in control parameters, the phase boundaries with different nonzero magnetic polarizations are first order near absolute zero and first-order transitions change into continuous transitions at a few Kelvin. Superconductivity is commonly induced or enhanced near these phase boundaries. The importance of the first-order line for superconductivity in  $\text{UGe}_2$  has also been suggested from the enhancement of superconductivity at the field-induced FM1-FM2 phase transition.<sup>23,24)</sup> Contrary to  $\text{URhGe}$  and  $\text{UTe}_2$ , the connection between superconductivity and magnetic fluctuations does not hold experimentally in  $\text{UGe}_2$ . The electronic specific heat and the

\*kotegawa@crystal.kobe-u.ac.jp

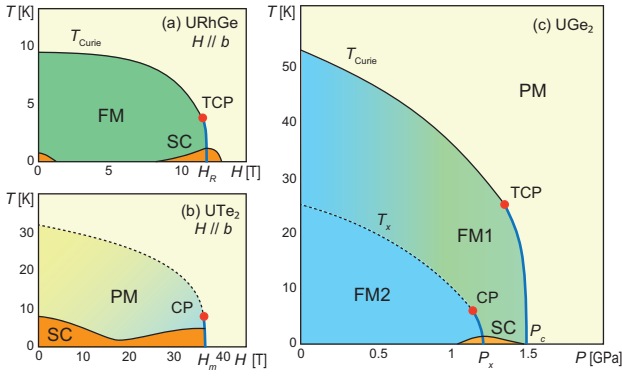


**Fig. 1.** (Color online) Magnetic field-temperature phase diagrams of (a) URhGe and (b) UTe<sub>2</sub>,<sup>4,7,8,13,21</sup> which are analogous to UGe<sub>2</sub>. (c) Pressure-temperature phase diagram of UGe<sub>2</sub>.<sup>1,32</sup> In UGe<sub>2</sub>, a second-order FM transition at  $T_{\text{Curie}}$  changes into a first order at a tricritical point (TCP) by applying pressure, and reaches 0 K at  $P_c$ . Likewise, the crossover between the FM1 and FM2 phases changes into first order at a critical point (CP), and reaches 0 K at  $P_x$ . In URhGe and UTe<sub>2</sub>, the magnetic fields induce the field-induced magnetically polarized phase through first-order phase transitions. These first-order lines are represented by blue curves. The solid black curves and the dotted black curves show the second-order lines and the crossover, respectively. In all three systems, superconductivity is induced or enhanced on the first-order quantum phase transition between two phases with different nonzero magnetic polarizations. Here, SC shows the superconducting (SC) phase and the SC transition temperatures are multiplied by arbitrary factors.

nuclear spin - lattice relaxation rate,  $1/T_1$ , do not show divergent behavior when the pressure crosses  $P_x$ .<sup>25,26</sup> Instead, step-like changes, similar to ordinary first-order transitions, are observed. In the case of electron-electron scattering in resistivity, that is, the  $A$  coefficient, two groups have reported different behavior. One report shows the step-like behavior as well as the aforementioned quantities,<sup>27</sup> while another report indicates that  $A$  shows the maximum near  $P_x$ ,<sup>28</sup> therefore, intrinsic behavior remains unclear. Most observations have not shown any remarkable anomaly near  $P_x$ , although superconductivity is clearly prominent there.<sup>29–31</sup> More significantly,  $1/T_1$  has not detected magnetic fluctuations expected at a critical point (CP),<sup>26</sup> which has been reported to be at 1.15 GPa and 7 K.<sup>32</sup> There was obvious experimental discrepancy between UGe<sub>2</sub> and other FM superconductors, therefore, the origin of superconductivity induced in UGe<sub>2</sub> remained unknown. At present, UGe<sub>2</sub> is a key ingredient to reach consensus on superconductivity induced by FM fluctuations.

To address this issue of UGe<sub>2</sub>, in this Letter, we focus on the spin-echo decay rate,  $1/T_2$ , which has not yet been reported. This rate includes magnetic fluctuations along the nuclear quantization axis, which is in contrast to  $1/T_1$  that corresponds to magnetic fluctuations perpendicular to the axis. It has already been demonstrated that the evaluation of magnetic fluctuations using  $1/T_2$  is effective in URhGe.<sup>14,17,18</sup> In the magnetically ordered state, the nuclear quantization axis is directed along the internal field under the condition that the nuclear Zeeman interaction is predominant over the nuclear quadrupole interaction. In UGe<sub>2</sub>, this situation is approximately realized and the internal fields at the Ge sites are directed along the  $a$ -axis (see the supplemental materials).<sup>33</sup> Therefore, it can be interpreted that  $1/T_2$  corresponds to longitudinal magnetic fluctuations and  $1/T_1$  corresponds to transverse magnetic fluctuations. We observed that  $1/T_2$  is

strongly enhanced near the FM1-FM2 boundary, in contrast to  $1/T_1$ , revealing that anisotropic magnetic fluctuations underlie the occurrence of superconductivity in UGe<sub>2</sub>.

The samples for our study were made using enriched <sup>73</sup>Ge for NMR measurements. We used a polycrystalline sample and a single crystal grown by the Czochralski method. Both samples were crushed into powder, to obtain reasonable intensity of the <sup>73</sup>Ge-NMR signal, and then annealed to reduce possible deformation. NMR data show no difference between the polycrystalline sample and crushed single crystal; therefore, we do not distinguish them in this Letter. NMR measurements were performed using the conventional spin-echo method. Pressure was applied using a piston cylinder cell and Daphne7474 was used as a pressure transmitting medium.<sup>34</sup> Pressure calibration was done from the superconducting transition temperature of a Pb manometer.

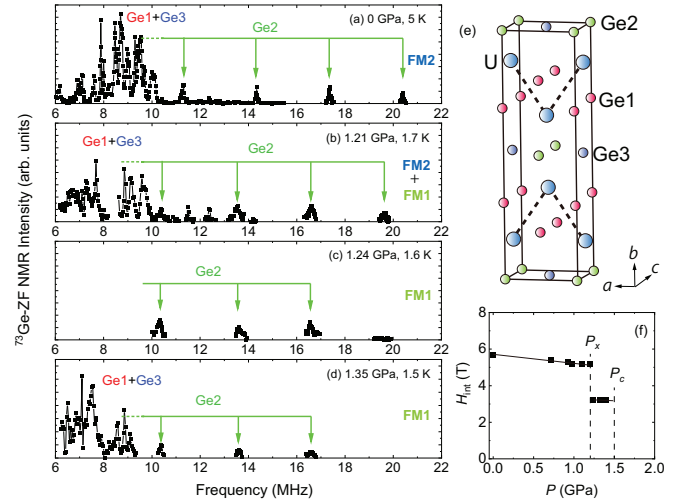


**Fig. 2.** (Color online) (a-d) ZF-NMR spectra in the FM states of UGe<sub>2</sub>. The spectrum at ambient pressure is identical to that reported in Ref.<sup>35</sup> The resonance lines for the Ge2 sites are well separated by the quadrupole interaction, whereas many transitions from the Ge1 and Ge3 sites are overlapped in the range below  $\sim 10$  MHz. (e) The crystal structure of UGe<sub>2</sub> and three inequivalent Ge sites. (f) The pressure dependence of the internal field for the Ge2 site at  $\sim 1.6$  K. The solid lines are drawn as guidelines.

Figure 2 shows zero field (ZF)-NMR spectra in the FM state for UGe<sub>2</sub> at several pressures. UGe<sub>2</sub> crystallizes in the orthorhombic structure in  $Cmmm$  space group and includes three Ge sites, denoted as Ge1, Ge2, and Ge3. Since the nuclear spin of <sup>73</sup>Ge is  $I = 9/2$ , each Ge site provides 9 spectral lines in the Zeeman interaction. The resonance lines from the Ge2 sites are well separated, while many transitions are overlapped for the Ge1 and Ge3 sites because the directions of the principal axes of the electric field gradient (EFG) with respect to the internal field along the  $a$ -axis are different among them.<sup>33,35</sup> The resolvable lines of the Ge2 site enable us to separately estimate the internal field and the quadrupole frequency. The signals for Ge2 site were undetected in previous studies under pressure.<sup>26,36,37</sup> The signal observed at  $\sim 20.3$  MHz at ambient pressure (the FM2 phase) is the high-frequency end of the resonance lines for the nuclear spin  $I = 9/2$ . At 1.24 GPa (the FM1 phase), the high-frequency end suddenly moves to  $\sim 16.6$  MHz due to discrete reduction

of the ordered moment. The pressure dependence of the internal field is shown in Fig. 2(f), which is consistent with the pressure dependence of the ordered moment.<sup>38)</sup> Near  $P_x$ , the phase separation of the FM1-FM2 phases is known to occur owing to the first-order transition.<sup>26,37)</sup> In Fig. 2(b), for example, it is suggested that the signals at  $\sim 7.7$  MHz and  $\sim 9.6$  MHz are attributed to the FM2 phase and that the signal below  $\sim 7$  MHz originates in the FM1 phase.<sup>37)</sup> The considerable intensity near 20 MHz also shows that the FM2 phase remains at 1.21 GPa. In the vicinity of  $P_x$ , as shown in Figs. 2(b) and (c), the satellite lines of the Ge2 site are observed at a similar position between the FM1 and FM2 phases.

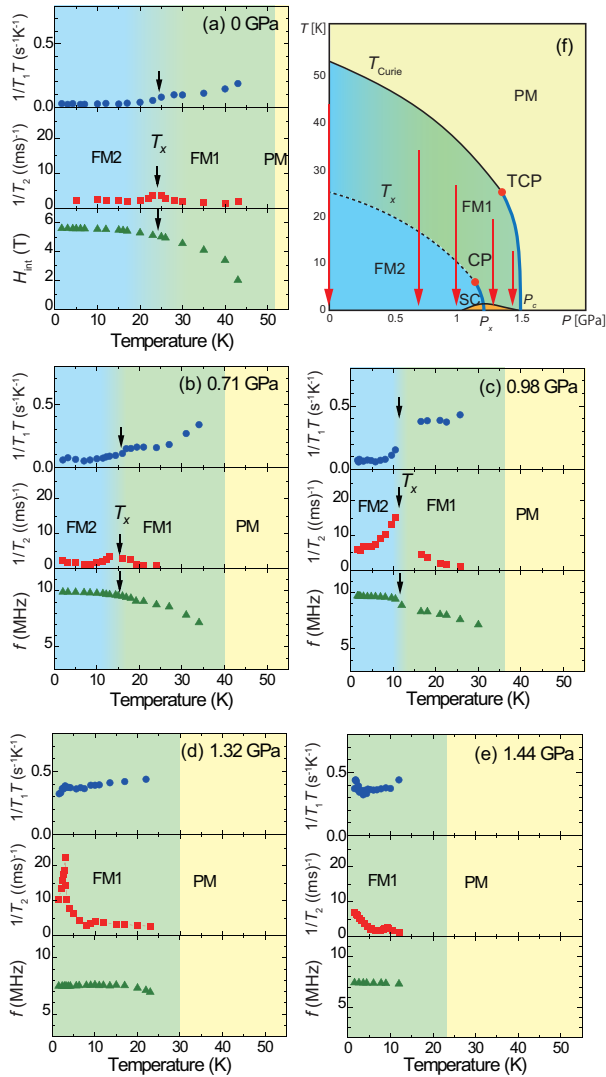


**Fig. 3.** (Color online) (a-e) Temperature dependences of  $1/T_1T$ ,  $1/T_2$ , and the internal field (resonance frequency) measured at several pressures. (f) The arrows in the phase diagram show the pressures where the measurements were performed. (a) At ambient pressure, the data were measured at the Ge2 site.  $1/T_1T$  and the internal field have been reported in Ref.<sup>35)</sup> (b-e) Under pressure, both relaxation rates were measured at the resonance frequencies shown in each bottom figure, which is expected to be the Ge1 site.<sup>33)</sup>  $1/T_1T$  shows a gradual decrease below  $T_x$  as well as in previous studies.<sup>26,37)</sup>  $1/T_2$  shows obvious divergence near  $T_x$ , which is remarkable at 0.98 GPa near the CP. The peak in  $1/T_2$  remains at 1.32 GPa, where the phase transition does not occur in the FM phase. The estimation of the internal field under pressure are shown in the supplemental materials.<sup>33)</sup>

The temperature dependences of  $1/T_1T$ ,  $1/T_2$ , and the internal field at the Ge site (or the resonance frequency) are summarized in Figs. 3(a-e). Here, the relaxation rates under pressure were measured at the signals expected to be the Ge1 sites,<sup>33)</sup> as from previous measurements of  $1/T_1T$ ,<sup>26,37)</sup> because the intensity of the Ge2 site was not strong enough at high temperatures.  $T_1$  was evaluated by fitting the recovery curve into theoretical curve for the central line of  $I = 9/2$  for convenience, although the many transitions seem to be overlapped. The site assignment for the Ge1 and Ge3 sites are shown in the supplemental materials.<sup>33)</sup> It roughly reproduces the spectrum, but uncertainty remains; therefore, the resonance frequencies are plotted in Figs. 3(b-d) instead of the internal field. At ambient pressure,  $1/T_1T$  shows a gradual decrease below a crossover temperature,  $T_x$ ,<sup>35)</sup> whereas  $1/T_2$  exhibits a small peak at  $T_x$ . Similar behavior is observed at 0.71 GPa and  $1/T_1T$  shows a smooth change at around  $T_x$ . At 0.98 GPa,  $T_1$  and  $T_2$  were hardly measurable near  $T_x$  owing to small intensity caused by short  $T_2$ . As shown in Fig. 3(c),  $1/T_2$  shows a clear increase around  $T_x$ . Such distinct enhancement is not seen in  $1/T_1T$ , as already confirmed in previous works.<sup>26,37)</sup> At 0.98 GPa, the resonance frequency,  $f$ , shows a clear change, like a phase transition, at  $T_x$ , which is consistent with the magnetization.<sup>39)</sup> This indicates that the magnetic fluctuations detected by  $1/T_2$  are enhanced when the crossover line is about to reach the CP.

Figures 3(d) and (e) show the data above  $P_x$ , where the magnetic ground state is the FM1 phase. In this pressure region,  $1/T_1T$  is almost temperature independent while the enhancement of  $1/T_2$  remains. At 1.32 GPa, just above  $P_x$ , a clear peak appears in  $1/T_2$  at  $\sim 3$  K, even though a crossover or a phase transition no longer occurs. This result clearly suggests that the origin of fluctuations, or the CP, is located at a nonzero temperature. This is qualitatively consistent with the suggestion by the resistivity measurement.<sup>32)</sup> It should be noted that this fluctuation has been overlooked in previous NMR measurements, which focused on  $1/T_1T$ .<sup>26,37)</sup> The difference between  $1/T_2$  and  $1/T_1T$  indicates that the magnetic fluctuations are highly anisotropic. This is common behavior for systems in which longitudinal magnetic fluctuations are significantly strong, as seen near the CP of the metamagnetic transition of UCoAl.<sup>40,41)</sup>

Conclusive evidence for the connection between the first-order line and the anomaly in  $1/T_2$  is given by its pressure dependence at the low temperature of  $\sim 1.6$  K, which is shown in Fig. 4. Here, the data at the Ge2 site (red) and the possible Ge1 site (blue) are plotted. The measurement at the Ge2 site further validates the quantitative comparison of  $1/T_2$ , because the spectrum is well-separated. The spin-echo decay curves are shown in the supplemental materials.<sup>33)</sup> The results for both sites demonstrate that  $1/T_2$  is enhanced near the first-order line,<sup>42)</sup> which is connected to the CP. Such clear behavior was not observed in  $1/T_1T$ .<sup>26,37)</sup> The maxima in  $1/T_2$  are obtained at  $\sim 1.2$  GPa, where the phase separation occurs. It is meaningful to clarify which of the FM1 or FM2 phase provides the maximum in  $1/T_2$ , but it is difficult to conclude it. For the possible Ge1 site, the maximum in  $1/T_2$  was obtained at  $\sim 7.51$  MHz. It is likely to be the FM1 phase, but the spectrum is not well-resolved. The maximum for the Ge2 site was obtained at  $\sim 16.6$  MHz, wherein it is difficult to judge whether it is the FM1 or FM2 phase because they ap-



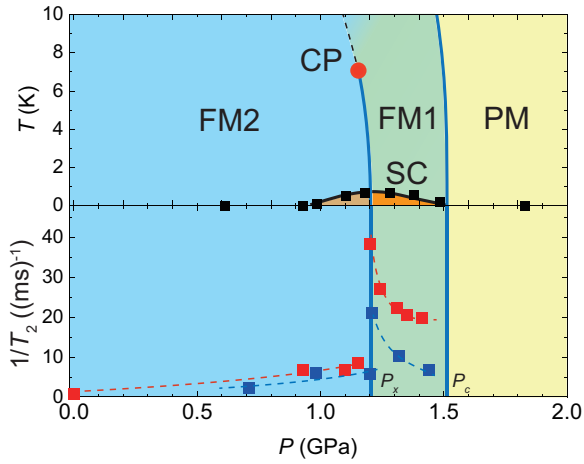


**Fig. 4.** (Color online) (top): Pressure-temperature phase diagram of UGe<sub>2</sub> near the SC phase. The position of the CP is cited from.<sup>32)</sup> The SC phase is drawn for that obtained by the resistivity measurements,<sup>1,25)</sup> whereas large jumps in the specific heat are obtained only in the vicinity of, or just above,  $P_x$ .<sup>29,31)</sup> (bottom): Pressure dependence of  $1/T_2$  measured at the Ge2 site (red) and at the possible Ge1 site (blue) at  $\sim 1.6$  K. The clear divergence of  $1/T_2$  is seen at the high-pressure side of  $P_x$ . The large specific heat jumps at  $T_{sc}$  and the enhancement of  $1/T_2$  are observed in a similar pressure region. The dotted curves are guides to the eye.

pear at similar frequencies, as mentioned above. In any case, the peaks of  $1/T_2$  were obtained just at  $P_x$ , and remarkably, the enhancement of  $1/T_2$  is not symmetric against pressure but prominent at the high-pressure FM1 side. This behavior in  $1/T_2$  is interesting when its pressure dependence is compared with superconductivity. Superconductivity has been observed as a dome shape in resistivity measurements,<sup>1,25)</sup> but large jumps in the specific heat are obtained only in the vicinity of, or just above,  $P_x$ .<sup>29,31)</sup> Regarding the superconductivity in the low-pressure FM2 phase, a realization that it is a bulk property has been controversial because of the smallness of the anomalies.<sup>30,31)</sup> In ZF-NMR in the FM2 phase, superconducting anomalies appear below a temperature significantly lower than  $T_{sc}$  estimated by resistivity.<sup>26,37)</sup> Many experiments have suggested that superconductivity of UGe<sub>2</sub> is prominent in the vicinity of, or in a narrow pressure region above  $P_x$ . This situation coincides with the interpretation that the longitudinal fluctuations observed in  $1/T_2$  is related to superconductivity. The relationship between superconductivity and magnetic fluctuations near  $P_x$  in UGe<sub>2</sub> has recently been suggested from analysis of magnetization data<sup>43)</sup> and our result is direct observation of the longitudinal magnetic fluctuations near  $P_x$ . We should also discuss the correspondence between the magnetic fluctuations observed in  $1/T_2$  and other macroscopic measurements. Our result seems to be qualitatively consistent with the  $A$  coefficient by Terashima *et al.*,<sup>28)</sup> although other resistivity data and electronic specific heat have not shown such an anomaly.<sup>25,27)</sup> We speculate that this discrepancy is caused by the inevitable phase separation of FM1 and FM2 phases. As seen in Fig. 4, the enhancement of magnetic fluctuations is realized in a narrow pressure region. If the FM2 phase, where the  $A$  coefficient and electronic specific heat are quite small,<sup>25,27,28)</sup> were mixed near  $P_x$  owing to the phase separation, the averaged quantities will depend on the volume fraction of each phase and detection of the anomaly would hardly be possible.

In conclusion, we have performed  $^{73}\text{Ge}$ -NMR measurements to address magnetic fluctuations in the vicinity of the first-order FM1-FM2 phase boundary at  $P_x$ . Using the spin-echo decay rate  $1/T_2$ , we extracted the longitudinal magnetic fluctuations and revealed that they develop near the CP. The magnetic fluctuations, which most likely originate in the CP, survive at low temperatures, and its pressure dependence shows divergent behavior near  $P_x$ . The fluctuations are remarkable in a narrow pressure region on the high-pressure side of  $P_x$ , where the SC anomaly has been clearly observed in the specific heat. The present result suggests that the connection of magnetic fluctuations and superconductivity is also underlying in UGe<sub>2</sub>, as well as in other FM superconductors. This finding will strongly promote unified understanding of Cooper-pair formation in magnetized materials.

**Acknowledgment** We thank K. Ishida, M. Manago, Y. Tokunaga, V. Taufour, and J. Flouquet for helpful discussions, and E. E. Haller for experimental support. This work was supported by JSPS KAKENHI Grants (Nos. 15H05885, 15H05882, 18H04321 (J-Physics), and 15H05745).

- 1) S. S. Saxena, P. Agarwal, K. Ahilan, F. M. Grosche, R. K. W. Haselwimmer, M. J. Steiner, E. Pugh, I. R. Walker, S. R. Julian, P. Monthoux, G. G. Lonzarich, A. Huxley, I. Sheikin, D. Braithwaite, and J. Flouquet, *Nature (London)* **406**, 587 (2000).
- 2) D. Aoki, A. Huxley, E. Ressouche, D. Braithwaite, J. Flouquet, J.-P. Brison, E. Lhotel, and C. Paulsen, *Nature (London)* **413**, 613 (2001).
- 3) N. T. Huy, A. Gasparini, D. E. de Nijs, Y. Huang, J. C. P. Klaasse, T. Gortenmulder, A. de Visser, A. Hamann, T. Görlach, and H. v. Löhneysen, *Phys. Rev. Lett.* **99**, 067006 (2007).
- 4) F. Lévy, I. Sheikin, B. Grenier, and A. D. Huxley, *Science* **309**, 1343 (2005).
- 5) D. Aoki, T. D. Matsuda, V. Taufour, E. Hassinger, G. Knebel, and J. Flouquet, *J. Phys. Soc. Jpn.* **78**, 113709 (2009).
- 6) S. Ran, C. Eckberg, Q.-P. Ding, Y. Furukawa, T. Metz, S. R. Saha, I.-L. Liu, M. Zic, H. Kim, J. Paglione, and N. P. Butch, *Science* **365**, 684 (2019).
- 7) G. Knebel, W. Knafo, A. Pourret, Q. Niu, M. Valiska, D. Braithwaite, G. Lapertot, M. Nardone, A. Zitouni, S. Mishra, I. Sheikin, G. Seyfarth, J.-P. Brison, D. Aoki, and J. Flouquet, *J. Phys. Soc. Jpn.* **88**, 063707 (2019).
- 8) S. Ran, I.-L. Liu, Y. S. Eo, D. J. Campbell, P. M. Neves, W. T. Fuhrman, S. R. Saha, C. Eckberg, H. Kim, D. Graf, F. Balakirev, J. Singleton, J. Paglione, and N. P. Butch, *Nature Physics* **15**, 1250 (2019).
- 9) D. Aoki, K. Ishida, and J. Flouquet, *J. Phys. Soc. Jpn.* **88**, 022001 (2019).
- 10) A. D. Huxley, *Physica C* **514**, 368 (2015).
- 11) T. Hattori, Y. Ihara, Y. Nakai, K. Ishida, Y. Tada, S. Fujimoto, N. Kawakami, E. Osaki, K. Deguchi, N. K. Sato, and I. Satoh, *Phys. Rev. Lett.* **108**, 066403 (2012).
- 12) D. Fay and J. Appel, *Phys. Rev. B* **22**, 3173 (1980).
- 13) D. Aoki, G. Knebel, and J. Flouquet, *J. Phys. Soc. Jpn.* **83**, 094719 (2014).
- 14) H. Kotegawa, K. Fukumoto, T. Toyama, H. Tou, H. Harima, A. Harada, Y. Kitaoka, Y. Haga, E. Yamamoto, Y. Ōnuki, K. M. Itoh, and E. E. Haller, *J. Phys. Soc. Jpn.* **84**, 054710 (2015).
- 15) A. Gourgout, A. Pourret, G. Knebel, D. Aoki, G. Seyfarth, and J. Flouquet, *Phys. Rev. Lett.* **117**, 046401 (2016).
- 16) S. Nakamura, T. Sakakibara, Y. Shimizu, S. Kittaka, Y. Kono, Y. Haga, J. Pospisil, and E. Yamamoto, *Phys. Rev. B* **96**, 094411 (2017).
- 17) Y. Tokunaga, D. Aoki, H. Mayaffre, S. Krämer, M.-H. Julien, C. Berthier, M. Horvatić, H. Sakai, S. Kambe, and S. Araki, *Phys. Rev. Lett.* **114**, 216401 (2015).
- 18) Y. Tokunaga, D. Aoki, H. Mayaffre, S. Krämer, M.-H. Julien, C. Berthier, M. Horvatić, H. Sakai, T. Hattori, S. Kambe, and S. Araki, *Phys. Rev. B* **93**, 201112(R) (2016).
- 19) A. Miyake, D. Aoki, and J. Flouquet, *J. Phys. Soc. Jpn.* **77**, 094709 (2008).
- 20) F. Hardy, D. Aoki, C. Meingast, P. Schweiss, P. Burger, H. v. Löhneysen, and J. Flouquet, *Phys. Rev. B* **83**, 195107 (2011).
- 21) W. Knafo, M. Valiska, D. Braithwaite, G. Lapertot, G. Knebel, A. Pour-

- ret, J.-P. Brison, J. Flouquet, and D. Aoki, J. Phys. Soc. Jpn. **88**, 063705 (2019).
- 22) A. Miyake, Y. Shimizu, Y. J. Sato, D. Li, A. Nakamura, Y. Homma, F. Honda, J. Flouquet, M. Tokunaga, and D. Aoki, J. Phys. Soc. Jpn. **88**, 063706 (2019).
  - 23) A. Huxley, I. Sheikin, E. Ressouche, N. Kernavanois, D. Braithwaite, R. Calemczuk, and J. Flouquet, Phys. Rev. B **63**, 144519 (2001).
  - 24) I. Sheikin, A. Huxley, D. Braithwaite, J. P. Brison, S. Watanabe, K. Miyake, and J. Flouquet, Phys. Rev. B **64**, 220503(R) (2001).
  - 25) N. Tateiwa, T. C. Kobayashi, K. Hanazono, K. Amaya, Y. Haga, R. Settai, and Y. Ōnuki, J. Phys.: Condens. Matter **13**, L17 (2001).
  - 26) H. Kotegawa, A. Harada, S. Kawasaki, Y. Kitaoka, Y. Haga, E. Yamamoto, Y. Ōnuki, K. M. Itoh, E. E. Haller, and H. Harima, J. Phys. Soc. Jpn. **74**, 705 (2005).
  - 27) T. C. Kobayashi, K. Hanazono, N. Tateiwa, K. Amaya, Y. Haga, R. Settai, and Y. Ōnuki, J. Phys.: Condens. Matter **14**, 10779 (2002).
  - 28) T. Terashima, K. Enomoto, T. Konoike, T. Matsumoto, S. Uji, N. Kimura, M. Endo, T. Komatsubara, H. Aoki, and K. Maezawa, Phys. Rev. B **73**, 140406(R) (2006).
  - 29) N. Tateiwa, T. C. Kobayashi, K. Amaya, Y. Haga, R. Settai, and Y. Ōnuki, Phys. Rev. B **69**, 180513(R) (2004).
  - 30) N. Kabeya, R. Iijima, E. Osaki, S. Ban, K. Imura, K. Deguchi, N. Aso, Y. Homma, Y. Shiokawa, and N. K. Sato, Physica B **404**, 3238 (2009).
  - 31) V. Taufour, PhD thesis: <https://tel.archives-ouvertes.fr/tel-00639652>
  - 32) V. Taufour, D. Aoki, G. Knebel, and J. Flouquet, Phys. Rev. Lett. **105**, 217201 (2010).
  - 33) (Supplemental material) The site assignment for the Ge1 and Ge3 sites, the estimation of the internal field at the possible Ge1 site, and the spin-echo decay for  $T_2$  measurements are provided online.
  - 34) K. Murata, K. Yokogawa, H. Yoshino, S. Klotz, P. Munsch, A. Irizawa, M. Nishiyama, K. Iizuka, T. Nanba, T. Okada, Y. Shiraga, and S. Aoyama, Rev. Sci. Instrum. **79**, 085101 (2008).
  - 35) Y. Noma, H. Kotegawa, T. Kubo, H. Tou, H. Harima, Y. Haga, E. Yamamoto, Y. Ōnuki, K. M. Itoh, E. E. Haller, A. Nakamura, Y. Homma, F. Honda, and D. Aoki, J. Phys. Soc. Jpn. **87**, 033704 (2018).
  - 36) A. Harada, S. Kawasaki, H. Kotegawa, Y. Kitaoka, Y. Haga, E. Yamamoto, Y. Ōnuki, K. M. Itoh, E. E. Haller, and H. Harima, J. Phys. Soc. Jpn. **74**, 2675 (2005).
  - 37) A. Harada, S. Kawasaki, H. Mukuda, Y. Kitaoka, Y. Haga, E. Yamamoto, Y. Ōnuki, K. M. Itoh, E. E. Haller, and H. Harima, Phys. Rev. B **75**, 140502(R) (2007).
  - 38) C. Pfleiderer and A. D. Huxley, Phys. Rev. Lett. **89**, 147005 (2002).
  - 39) N. Tateiwa, K. Hanazono, T. C. Kobayashi, K. Amaya, T. Inoue, K. Kindo, Y. Koike, N. Metoki, Y. Haga, R. Settai, and Y. Ōnuki, J. Phys. Soc. Jpn. **70**, 2876 (2001).
  - 40) H. Nohara, H. Kotegawa, H. Tou, T. D. Matsuda, E. Yamamoto, Y. Haga, Z. Fisk, Y. Ōnuki, D. Aoki, and J. Flouquet, J. Phys. Soc. Jpn. **80**, 093707 (2011).
  - 41) K. Karube, T. Hattori, K. Ishida, and N. Kimura, Phys. Rev. B **91**, 075131 (2015).
  - 42) The spin-echo decay rate  $1/T_2$  corresponds to the fluctuations of the resonance frequency induced by the fluctuation of the internal field. The difference in  $1/T_2$  between the Ge2 site and the possible Ge1 site are considered to originate in the difference in the sensitivity of the resonance frequency to the internal field. In fact,  $\Delta f/\Delta H_{\text{int}}$  is estimated to be 1.55 MHz/T for the Ge2 site, and 1.27 MHz/T for the possible Ge1 site.
  - 43) N. Tateiwa, Y. Haga, and E. Yamamoto, Phys. Rev. Lett. **121**, 237001 (2018).